

# **Augmented Plane-Wave Method for Photonic Band-Gap Materials**

*W. C. Sailor and F. M. Mueller*

*Los Alamos National Laboratory*

*Los Alamos, NM 87545*

*Pierre R. Villeneuve*

*Massachusetts Institute of Technology*

*Cambridge, MA 02139*

## **Abstract**

We present a numerical method for computing the eigenstates of a photonic band-gap material based on the augmented plane-wave method. The method uses a functional basis set well suited for structures with spherical and cylindrical elements, and allows for fast numerical convergence with a small number of expansion terms. In addition, the method has the ability of dealing with both metallic and dielectric elements without special treatment. The method is applied to an array of long parallel rods with circular cross section.

Photonic crystals are man-made materials that have a periodicity in the dielectric constant.<sup>1</sup> They may be manufactured from a variety of materials and may possess a photonic band-gap (PBG). The first successfully predicted structure to yield a PBG was that of dielectric

spheres arranged in a diamond lattice.<sup>2</sup> Since then, there has been considerable effort to elaborate a process for the manufacturing of diamond (or diamond-like) structures at submicron wavelengths. One such approach consists in etching a large number of hole triplets at off-vertical angles in a slab.<sup>3</sup> Another consists in building an orderly stacking of dielectric rods.<sup>4</sup> Yet another consists in etching a series of horizontal grooves into sequentially-grown layers, and etching vertical holes.<sup>5</sup> These structures are variations of the same diamond structure, aligned along either the (1,1,1), (0,0,1), or (1,1,0) directions, respectively. In theoretical treatments, the plane-wave expansion method is commonly used for the computation of band structures and eigenfunctions.<sup>6</sup> However, simple structures such as the ones listed above are amenable to special theoretical treatment. By properly choosing the functional basis set, numerical convergence can be reached with a very small number of expansion terms.

In this paper, we present a theoretical method which uses a functional basis set particularly well suited for structures with spherical and cylindrical elements. Our computational method, based on the augmented plane-wave (APW) method of Slater,<sup>7</sup> uses Bessel functions as a basis set. The method was originally developed for electronic systems, and is usually applied to spherically-symmetric systems with scalar boundary conditions.<sup>8,9</sup> When applied to photonic band-gap materials, the APW method with Bessel functions is most suitable for structures with curved surfaces, and leads to vector boundary conditions.

In addition to yielding fast convergence, the APW method also has the ability of handling different types of materials. Conducting elements had been known to require special theoretical treatment, and several different computational schemes had been used to compute their photonic band structure.<sup>10</sup> However, the APW method can handle metallic elements equally as well as dielectric ones. In this letter, we focus our attention on periodic arrays of long parallel dielectric rods and long conducting rods positioned on a square

lattice. For these structures, the fields can be decomposed into two orthogonal polarizations, and the vector boundary conditions can be reduced to scalar conditions.

The Wigner-Seitz unit cell of the periodic array of rods is shown in Figure 1. In Region I, the basis functions  $\psi_i$  ( $i = 1, 2, \dots, n$ ) are given by Bessel functions  $J_m(x)$  and  $Y_m(x)$ , while in Region II, the basis functions are plane waves. Region I is chosen to extend beyond the edges of the cylindrical rod. By adjusting its dimension, we can maximize convergence depending on the geometry of the photonic crystal and the size of the rods. At the interface between Regions I and II, continuity is maintained by matching the Bessel functions to the plane waves using the following Laurent series:

$$e^{ik \cdot x} = \sum_{m=-\infty}^{\infty} i^m J_m(|k|x) e^{im(\theta - \phi)} \quad (1)$$

While Eq. (1) guarantees continuity of the wavefunction, it does not guarantee continuity of its derivative.

We convert the electromagnetic wave equation with periodic boundary conditions into a variational problem. The problem reduces to solving a non-linear eigenvalue equation of the form  $\det(M) = 0$ . The matrix elements  $M^{ij}$  are given by:

$$M^{ij} = H^{ij} + S^{ij} - \epsilon_j \delta^{ij} \quad (2)$$

where

$$H^{ij} = \int_{\Omega} \psi_i^* H \psi_j d\Omega \quad (3)$$

$$H_{ij} = - \int_{\Omega} \nabla \cdot \left( \frac{1}{\epsilon(\mathbf{r})} \nabla \phi_i^* \nabla \phi_j \right) d\mathbf{r} \quad (4)$$

$$S_{ij} = - \int_{\partial \Omega} \left( \frac{1}{\epsilon(\mathbf{r})} \nabla \phi_i^* \cdot \mathbf{n} - \frac{1}{\epsilon(\mathbf{r})} \nabla \phi_j \cdot \mathbf{n} \right) ds \quad (5)$$

The integration domain  $\Omega$  in Eqs. (3) and (4) corresponds to the total area of the unit cell defined by Regions I and II. In the first integral, the Hamiltonian operator  $H$  is given by  $-\nabla^2 + [1 - \epsilon(\mathbf{r})]$  where  $\epsilon(\mathbf{r})$  is the position-dependent dielectric function. The integral in Eq. (5) is a line integral along the edge of Region I.

By inserting the basis functions into the above equations, we find the following matrix elements

$$M_{ij}^{kl} = \frac{1}{4b^2(k_j^2 - k_i^2)} \left[ \frac{J_1(k_i b)}{k_i} - \frac{J_1(k_j b)}{k_j} \right] \cdot 2 \int_0^b J_m(k_i r) J_m(k_j r) \frac{R'_m(\sqrt{\epsilon} b)}{R_m(\sqrt{\epsilon} b)} \cos(m \theta) r dr \quad (6)$$

where  $R_m(x) = b_m J_m(x) + c_m Y_m(x)$  and  $R'_m(x)$  is the derivative of  $R_m(x)$  with respect to  $x$ . The quantities  $k_i$  and  $k_j$  are given by  $|k_j - k_i|$  and  $|k_j + k_i|$ , respectively, and the symbol  $\delta_{ij}$  represents the Kronecker delta function. In the case of loss-less isotropic media, the matrix is real and symmetric.

The coefficients  $b_m$  and  $c_m$  are chosen to satisfy the boundary conditions within Region I. The boundary conditions depend on the rod material and on the field polarization. In the case where the rods are made of dielectric material, the electric field is continuous at the surface for  $s$  polarization (electric field parallel to the rods) while for  $p$  polarization (magnetic field parallel to the rods) the magnetic field is continuous. In the case of

perfectly conducting rods, the field is zero at the surface for  $s$  polarization, and the derivative of the field is zero for  $p$  polarization.

We note that the eigenvalues in Eq. (6), which correspond to allowed frequencies, appear in a nonlinear manner. They are computed using a standard bisection root-finding routine for a fixed wavevector in the periodic lattice. For each  $k = (\pi/c)^2$  the determinant of the matrix  $M$  is found as the product of the diagonal elements in matrix  $U$ , which in turn is obtained by LU decomposition of matrix  $M$ . Special care must be taken in this procedure to avoid skipping over roots, especially when a pole in the determinant falls near a root. As a result of these types of difficulties, the accuracy of the calculations with the APW method depends on the amount of computing time one wishes to invest in finding these roots. For the calculations in this paper, the frequency domain was initially searched with 1000 equally-spaced points which gave an  $\omega$ -finding accuracy of six decimal places.

We computed the band diagram for two separate cases: (i) dielectric rods and (ii) metallic rods. In the case of dielectric rods, we choose a lattice constant  $2b$  of 1.0, a rod radius  $a$  of 0.2, and a dielectric material with an index of refraction of 3.4. Results for  $s$  polarization are shown in Fig. 2 for a  $2 \times 2$  and  $9 \times 9$  determinant. The results obtained from the plane-wave method developed at MIT<sup>11</sup> were found to have excellent agreement with the  $9 \times 9$  APW calculation and are not shown because the difference between the two sets of calculations is less than a line width.

In order to find the trend in the truncation error with the size of the basis set, the percent calculational convergence was computed for this structure at three different points in the Brillouin zone. The points were near the X point, the G point and the M point. The convergence is measured as the fractional error in the frequency versus the value from the  $49 \times 49$  calculation. As shown in Table 1, the convergence is extraordinarily good. For

example, both the s- and p-wave calculation is converged to better than 1% for the first eigenvalues when using only a single basis function. The 9x9 calculation is converged to four decimal places for the first four frequencies.

In the case of perfectly conducting rods, we choose a rod radius of 0.187 and a lattice constant of unity. Results for s polarized waves are shown in Fig. 3 for a 2x2 and 9x9 determinant. These results are to be compared with those presented in Fig. 6 of Ref. 12 where the Raleigh scattering method<sup>12</sup> is used with a 49x49 determinant. Again, excellent agreement can be found with 9 APW basis functions. Although the APW is similar to the Raleigh scattering method in the case of conductors, the higher rate of convergence of the APW method arises from the continuity conditions imposed at the boundary between Regions I and II.

An area that has been investigated by others for the purpose of determining photonic band structure accuracy is the effective long-wavelength dielectric constant ( $\epsilon_{\text{eff}}$ ) of the heterogeneous medium.<sup>13</sup> In our case we evaluated the first eigenvalue for the pure dielectric case of Figure 2 at  $\mathbf{k} = (2\pi)(0.05, 0)$ . If we were to follow the prescription of Ref. 13 we would plot the computed value of  $\epsilon_{\text{eff}}$  of versus N and allow N to go to infinity. However, it was found that using only a single basis function, the result was already converged to 5 decimal places. Any such plot would reflect only the noise in the calculational procedure, which is in the 6th decimal place.

Finally, the method described above can also be used to compute the band diagram of three-dimensionally periodic structures. For example, if additional rods are added in orthogonal or non-orthogonal directions, it may be possible to compute the band diagram of structures such as the one described in Refs. 4 and 5. Furthermore, since the APW method requires a small number of expansion terms to reach convergence, it is well suited

for the analysis of structures with very large dimensions, such as supercells containing multiple rods of various types, including defects.

The fast convergence of the APW method is due mostly to the excellent match between the basis set and the geometrical shape of the structure. In general, the APW method should prove to be very useful for a wide range of structures seeing that, in many cases, photonic band-gap materials have elements with cylindrical or spherical surfaces.

<b>Rank</b>	<b>k</b>	<b>Polar</b>	<b>Frequency Eigenvalue</b>				
			1	2	3	4	5
1x1		s	$4 \times 10^{-5}$	$2 \times 10^{-2}$	$4 \times 10^{-2}$		
9x9		s	$6 \times 10^{-7}$	$3 \times 10^{-5}$	$5 \times 10^{-5}$	$4 \times 10^{-5}$	$2 \times 10^{-4}$
25x25		s	$2 \times 10^{-7}$	$1 \times 10^{-7}$	$1 \times 10^{-7}$	0	$7 \times 10^{-7}$
1x1		p	$3 \times 10^{-3}$	$3 \times 10^{-3}$			
9x9		p	$1 \times 10^{-5}$	$2 \times 10^{-6}$	$4 \times 10^{-5}$	$4 \times 10^{-5}$	$9 \times 10^{-5}$
25x25		p	0	0	$8 \times 10^{-8}$	$2 \times 10^{-7}$	$3 \times 10^{-7}$
1x1	X	s	$9 \times 10^{-2}$	$2 \times 10^{-1}$			
9x9	X	s	$4 \times 10^{-5}$	$8 \times 10^{-5}$	$1 \times 10^{-4}$	$4 \times 10^{-4}$	$1 \times 10^{-5}$
25x25	X	s	0	$2 \times 10^{-7}$	$3 \times 10^{-7}$	$7 \times 10^{-7}$	$2 \times 10^{-7}$
1x1	X	p	$5 \times 10^{-2}$	$2 \times 10^{-1}$			
9x9	X	p	$2 \times 10^{-4}$	$2 \times 10^{-5}$	$5 \times 10^{-6}$	$7 \times 10^{-5}$	$2 \times 10^{-4}$
25x25	X	p	$5 \times 10^{-7}$	$7 \times 10^{-8}$	0	$2 \times 10^{-7}$	$2 \times 10^{-7}$
1x1	M	s	$3 \times 10^{-2}$	$4 \times 10^{-2}$			
9x9	M	s	$3 \times 10^{-5}$	$2 \times 10^{-4}$	$2 \times 10^{-4}$	$9 \times 10^{-5}$	$8 \times 10^{-4}$
25x25	M	s	$1 \times 10^{-7}$	$6 \times 10^{-7}$	$6 \times 10^{-7}$	$6 \times 10^{-7}$	$4 \times 10^{-6}$
1x1	M	p	$1 \times 10^{-2}$	$6 \times 10^{-2}$			
9x9	M	p	$5 \times 10^{-6}$	$2 \times 10^{-4}$	$2 \times 10^{-4}$	$2 \times 10^{-4}$	$3 \times 10^{-5}$
25x25	M	p	0	$5 \times 10^{-7}$	$5 \times 10^{-7}$	$1 \times 10^{-6}$	$7 \times 10^{-8}$

Table 1. Fractional convergence of the APW method as a function of the number of basis functions for the first five eigenvalues in the case of a two-dimensional lattice of dielectric rods. Shown are the results at three different points in the Brillouin zone and the two different polarizations.

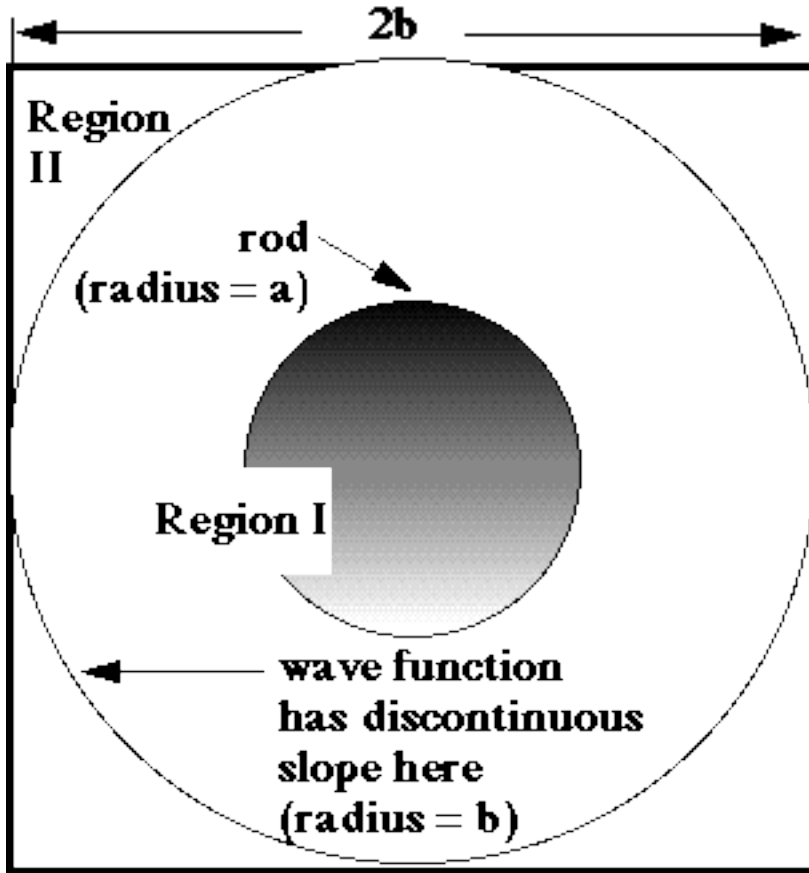


Fig. 1. Wigner-Seitz unit cell used in APW calculations. The rod region combined with the annular region concentric with the rod constitute Region I, where Bessel functions are used. The remaining volume is Region II, where free waves are used.



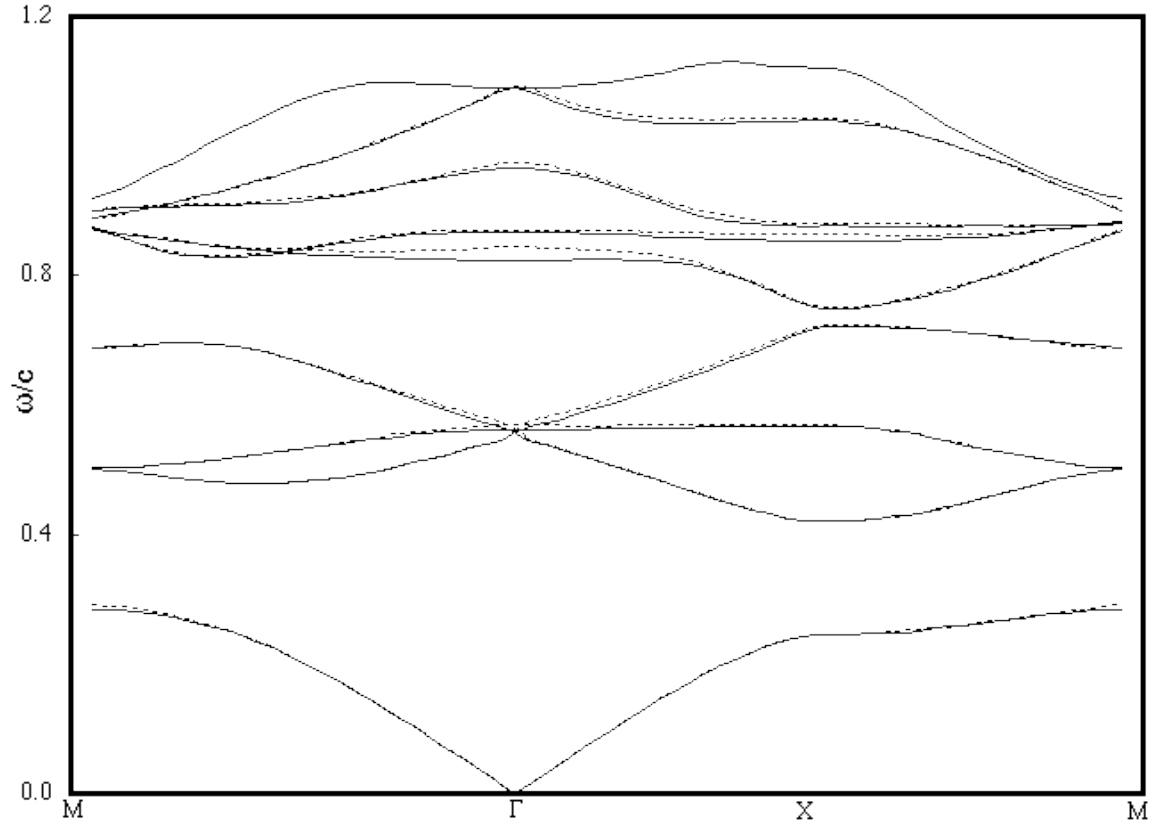


Fig. 2. Band diagram for  $s$ -polarized waves in an array of dielectric rods of index 3.4 computed with a 2x2 (dotted line) and 9x9 (solid line) determinant. The band diagram computed from the plane-wave method is not shown because it would be completely hidden below the 9x9 line. The rods have a radius of 0.2 and are located on a square lattice of unit length.

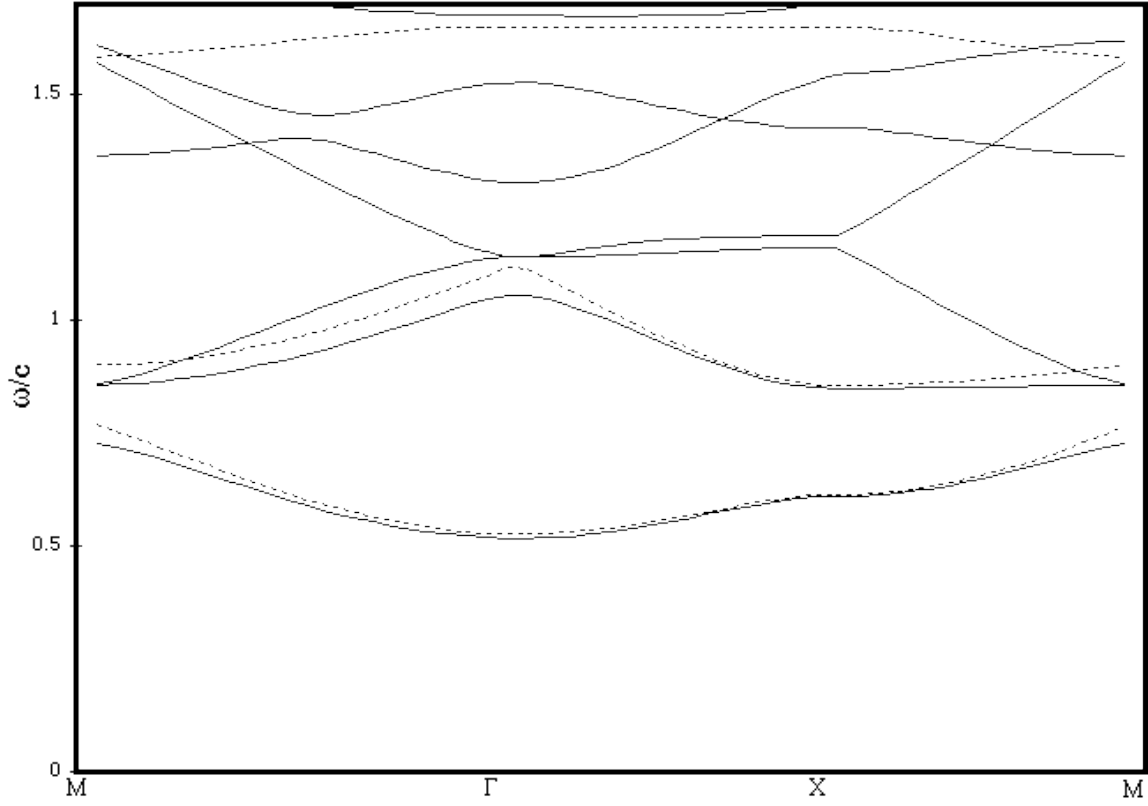


Fig. 3. Band diagram for  $s$ -polarized waves in an array of perfectly conducting rods computed with a 2x2 (dotted line) and 9x9 (solid line) determinant. The rods have a radius of 0.187 and are located on a square lattice of length 1. This is the same calculation as performed in Reference 12, Figure 6, by another method. The results are in excellent agreement.

## References

---

- <sup>1</sup> J. D. Joannopoulos, P. R. Villeneuve and S. Fan, *Nature* **386**, 143 (1997).
- <sup>2</sup> K. M. Ho, C. T. Chan, and C. M. Soukoulis, *Phys Rev. Lett.* **65**, 3152 (1990).
- <sup>3</sup> E. Yablonovitch, T. J. Gmitter, and K. M. Leung, *Phys. Rev. Lett.* **67**, 2295 (1991).
- <sup>4</sup> E. Ozbay, A. Abeyta, G. Tuttle, M. Tringedes, R. Biswas, C. T. Chan, C. M. Soukoulis, and K. M. Ho, *Phys. Rev. B* **50**, 1945 (1994).
- <sup>5</sup> S. H. Fan, P. R. Villeneuve, R. D. Meade, and J. D. Joannopoulos, *Appl. Phys. Lett.* **65**, 1466 (1994).
- <sup>6</sup> For a review, see P. R. Villeneuve and M. Piché, *Prog. Quant. Electr.* **18**, 153 (1994).
- <sup>7</sup> J. C. Slater, *Phys Rev.* **51**, 846 (1937).
- <sup>8</sup> L. F. Mattheiss, J. H. Wood, and A. C. Switendick, in *Methods In Computational Physics*, Edited by B. Alder, S. Fernbach, and M. Rotenberg (Academic Press, CITY, 1968).
- <sup>9</sup> T. L. Loucks, *Augmented Plane Wave Method, A Guide to Performing Electronic Structure Calculations* (Benjamin, New York, 1967).
- <sup>10</sup> See, for example, the Rayleigh scattering method: N. A. Nicorovici, R. C. McPhedran, and L. C. Botten, *Phys. Rev. Lett.* **75**, 1507 (1995); the transfer matrix method: J. B. Pendry, *J. Mod. Opt.* **41**, 109 (1994) and M. M. Sigalas, C. T. Chan, K. M. Ho, and C. M. Soukoulis, *Phys. Rev. B* **52**, 17744 (1995); the plane-wave method: A. R. McGurn and A. A. Maradudin, *Phys. Rev. B* **48**, 17576 (1993); and the finite-difference time-domain method: S. Fan, P. R. Villeneuve, and J. D. Joannopoulos, *Phys. Rev. B* **54**, 11245 (1996).
- <sup>11</sup> R. D. Meade, A. M. Rappe, K. D. Brommer, J. D. Joannopoulos, and O. L. Alerhand, *Phys Rev. B* **48**, 8434 (1993).
- <sup>12</sup> N. A. Nicorovici, R. C. McPhedran, and L. C. Botten, *Phys Rev. E* **52**, 1135 (1995).
- <sup>13</sup> H. S. Sozuer, J. W. Haus and R. Inguva, *Phys Rev B* **45** (1992) 13962.